Diagnostic of Silicon Carbide Surge Arresters of Substation

ARNALDO G. KANASHIRO[1] MILTON ZANOTTI JR.[1] PAULO F. OBASE[1]
WILSON R. BACEGA[2]
[1]University of São Paulo
Av. Prof. Luciano Gualberto, 1289, São Paulo / SP
[2]CTEEP – Companhia de Transmissão de Energia Elétrica Paulista
Rua Casa do Ator, 1155, São Paulo / SP
BRAZIL
arnaldo@iee.usp.br http://www.iee.usp.br

Abstract: - This paper presents the results of a research project aiming the diagnostic of the silicon carbide surge arresters. These surge arresters are being gradually replaced by the gapless zinc oxide ones, therefore, it is very important to select the surge arresters that are more degraded in order to avoid failures in the field. Tests were performed at the laboratory and the results showed a good correlation between the leakage current measurement, radio-influence voltage test and thermovision and the presence of deterioration in the internal parts of the surge arresters. The results obtained in this research might help the utility to develop more adequate maintenance programs and to select the silicon carbide surge arresters that need replacement.

Key-Words: - Diagnostic, Leakage Current, Radio-Influence, Silicon Carbide, Surge Arrester, Thermovision.

1 Introduction

The silicon carbide surge arresters (SiC) are being replaced by the zinc oxide (ZnO) ones [1,2], however, a large number of SiC are still in use in some utilities in Brazil. Due to the high costs, it is not possible to replace all the SiC surge arresters in a short term. Therefore, the two technologies of surge arresters remain installed in the Brazilian electrical system. It is important to emphasize that the SiC surge arresters presents 20 up to 25 years or more of service. As a consequence, the utilities have to review their maintenance program in order to guarantee a satisfactory performance until the SiC surge arresters are replaced [3,4]. In this context, a research project was established between the electrical utility CTEEP and the University of São Paulo, aiming at the diagnostic of the SiC surge arresters.

The first step of this research was to analyze the characteristics of the SiC surge arresters in service, considering their age, manufacturer, rated voltage, etc. Then, some of the SiC surge arresters were selected to be tested at the laboratory. The methodology of the investigation was based on the laboratory tests and visual inspection and tests of the internal components of disassembled surge arresters. Thirty-five SiC surge arresters of nominal voltages 88 kV, 138 kV, 230 kV, 345 kV and 440 kV, from five manufacturers, were considered.

The evaluation of the surge arresters was conducted at the IEE/USP High Voltage Laboratory. The following tests were performed: power frequency spark-over voltage, lightning spark-over voltage and leakage current measurement. Radio-influence voltage test (RIV) and thermovision were also performed in some arresters in order to have additional information of the internal components of the SiC surge arresters.

The values of the power frequency spark-over voltage and lightning spark-over voltage tests were compared to the requirements of the manufacturers and of the IEC standards [5]. Some of the surge arresters fulfilled the requirements, but the results of the leakage current measurement, radio-influence voltage test (RIV) and thermovision suggested that they presented a certain degree of deterioration nevertheless. Afterwards, a visual inspection and tests of the internal components of the surge arresters confirmed the assumption above.

The methodology adopted in this investigation allowed the comparison of the diagnostic techniques. The results of the leakage current measurements, one of the techniques used to evaluate the ZnO surge arresters [6,7,8], showed that it is also possible to apply this technique to the SiC, being obtained important information of their actual condition.

On the other hand, partial discharges are often a predecessor of serious fault in power transformers [9,10]. In this research, it was also used a promising technique to detect the presence of internal electrical discharges in the surge arresters. Tests were performed using a high frequency current transformer, in order to analyze the emission of the conducted electromagnetic field, from the SiC surge arresters. This technique was firstly developed to detect partial discharges in the potential and current transformers.

This paper shows the principal results of the investigation concerning the diagnostic of the SiC surge arresters. The results are related to the 88 and 138 kV surge arresters. Similar results were obtained with the 230 kV, 345 kV and 440 kV SiC surge arresters and are not shown in this paper. As a conclusion, a reasonable correlation was obtained between the results of the AC leakage current measurement, radio-influence voltage test and thermovision and the presence of deterioration of the SiC surge arresters.

2 Laboratory Tests

The SiC surge arresters selected to be tested at the laboratory were no longer being used by the utility in its electrical system. They were either replaced by ZnO surge arresters or presented abnormal heating during thermovision periodical measurements. In the laboratory, it was observed that almost all of the SiC surge arresters had some degree of corrosion in their metallic parts, as shown in Fig.1.

In some of the 88 kV surge arresters, discharge signs on the porcelain and on the metallic parts were noticed, as shown in Fig.2, indicating the occurrence of failure.

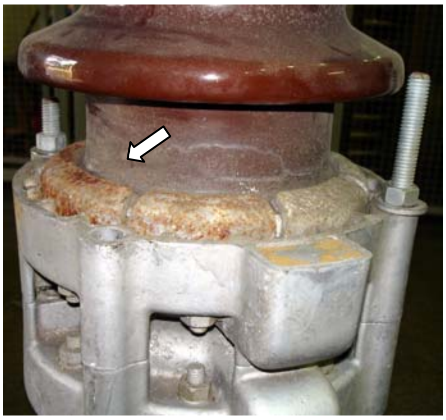

Fig.1 – Corrosion in the metallic parts of the surge arrester.

Therefore, prior to the laboratory tests, measurements of insulation resistance and of Watts losses, were carried out on several surge arresters, aiming at a preliminary check of their general condition.

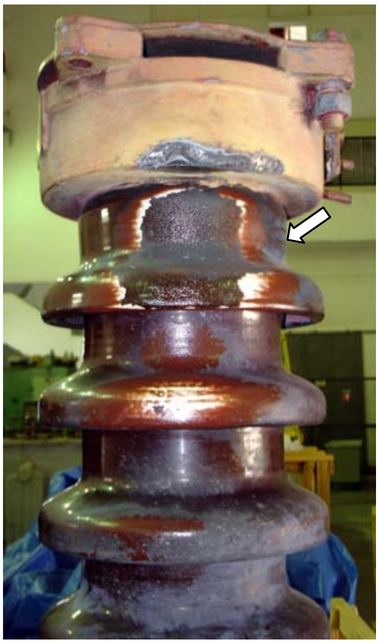

Fig.2 – Discharge signs on the porcelain and on the metallic parts of the surge arrester.

These SiC surge arresters operated during about 20 up to 25 years in the substations; however, there wasn't any information about their behaviour in all time period. Then, the values of the power frequency spark-over voltage and lightning spark-over voltage tests, obtained at the laboratory, were firstly used as reference to indicate changes taking into account the requirements of the manufacturers and of the IEC standards. Afterwards, the SiC surge arresters were submitted to the leakage current measurement, RIV and thermovision. A better diagnostic of the SiC surge arresters was obtained.

Table 1 and Table 2 show the results of the power frequency spark-over voltage and lightning spark-over voltage tests. According to the manufacturer's requirements, all 88 kV surge arresters failed the power frequency spark-over voltage test. In this test, A5 and A6 arresters presented unstable behaviour and it was not possible to determine their values of the power frequency spark-over voltage. The 138 kV surge arresters A7, A8, A9, C5, D3 and D5 failed the power frequency spark-over voltage test. Regarding the lightning spark-over voltage test, all surge arresters (88 kV and 138 kV) fulfilled the manufacturer's requirements.

Table 1: 88 kV surge arresters.

Manufacturer A	Power frequency spark-over voltage (kV)	Lightning spark-over voltage (kV)	
		Positive	Negative
A1	134	182	181
A2	105	171	168
A3	85	178	178
A4	102	172	167
A5	-----	173	172
A6	-----	173	188

Afterwards, measurements of the leakage current were carried out, with the amplitude (I_{peak}) and the third harmonic component (3^a H) being obtained. The phase difference between the leakage current and the voltage applied to the surge arrester was also determined. After the measurements above, RIV measurements, with frequency of 500 kHz and impedance of 300 Ω, and thermovision tests were performed considering some arresters.

The thermal image measurements were carried out after the surge arresters had been energized for a time period of 5 to 7.5 hours, depending on the manufacturer. One measurement was carried out for each of four different sides of the surge arrester. Each measurement corresponds to the thermal imaging obtained along the surge arrester, from top to bottom.

Each of the four sides of the sample had its maximum and minimum temperatures determined, and the difference (Δt) between these temperatures was calculated. The greatest difference value found was named "Δt_{max}". The highest temperature value obtained in the sample was named "t_{max}".

In the three tests mentioned before, the phase-to-ground voltages 51 kV and 80 kV were applied to the 88 kV and 138 kV samples, respectively. All the results obtained are shown in Table 3. The Fig. 3 shows an example of a thermal image measurement and the Fig. 4 shows the surge arrester submitted to the leakage current measurement.

Table 2: 138 kV surge arresters.

Manufacturers A/B/C/D	Power frequency spark-over voltage (kV)	Lightning spark-over voltage (kV)	
		Positive	Negative
A7	193	227	227
A8	170	222	228
A9	178	225	224
B1	244	284	272
B2	246	279	272
B3	242	287	294
B4	233	234	225
B5	237	234	229
B6	241	271	269
B7	232	272	272
C1	226	382	354
C2	219	374	363
C3	224	364	359
C4	218	340	322
C5	188	349	344
C6	233	355	344
D1	274	374	367
D2	273	376	372
D3	268	376	366
D4	271	372	369
D5	262	378	369

Table 3: Measurements of the leakage current, RIV and thermal image.

Manufacturers A/B/C/D	Power frequency spark-over voltage (kV)	Leakage current		Phase difference (degree)	RIV (μV)	Thermal image (^{0}C)	
		Peak value (mA)	3ª H (%)			t_{max}	Δt_{max}
A1	134 (R)	0.172	6.7	89	*	20.8	2.0
A2	105 (R)	0.192	10.1	65	**	21.6	2.0
A3	85 (R)	0.412	24.9	54	11	**	**
A4	102 (R)	0.696	32.9	47	29	**	**
A5	---- (R)	0.363	5.7	39	143	24.2	5.1
A6	---- (R)	0.384	5.0	67	8033	**	**
A7	193 (R)	0.278	2.6	85	*	29.3	7.0
A8	170 (R)	0.268	5.6	70	*	28.8	6.2
A9	178 (R)	0.246	6.8	71	36	**	**
B1	244	0.226	4.8	72	11	**	**
B2	246	0.252	5.7	70	25	28.0	4.6
B3	242	0.370	6.0	77	**	28.3	4.3
B4	233	0.234	6.4	68	25	**	**
B5	237	0.251	6.8	68	10	**	**
B6	241	0.230	8.5	63	25	27.9	4.4
B7	232	0.261	9.4	53	23	**	**
C1	226	0.363	5.6	73	23	**	**
C2	219	0.456	5.8	75	80	**	**
C3	224	0.346	6.8	79	*	19.9	2.6
C4	218	0.332	6.9	68	*	**	**
C5	188 (R)	0.430	7.5	83	4,518	19.3	2.8
C6	233	0.726	18	51	6,381	32.6	17.6
D1	274	0.364	1.9	89	*	18.1	1.7
D2	273	0.357	2.1	89	*	**	**
D3	268 (R)	0.357	2.1	82	64	18.2	1.9
D4	271	0.330	2.5	84	*	**	**
D5	262 (R)	0.331	3.8	78	90	**	**

(R) this surge arrester failed the power frequency spark-over voltage test.
(*) significant results were not observed in the RIV test.
(**) not tested.

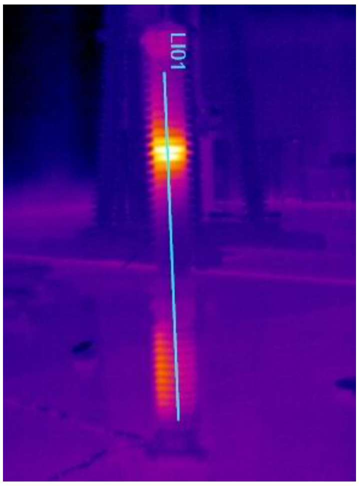

(a) thermal image of the surge arrester.

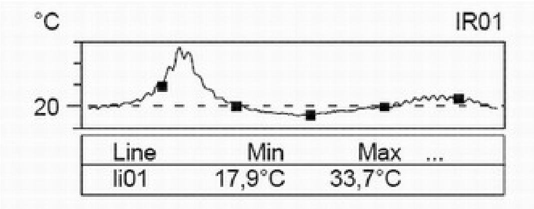

(b) temperature along the surge arrester.

Fig.3 – Thermal image along the surge arrester and the respective temperature.

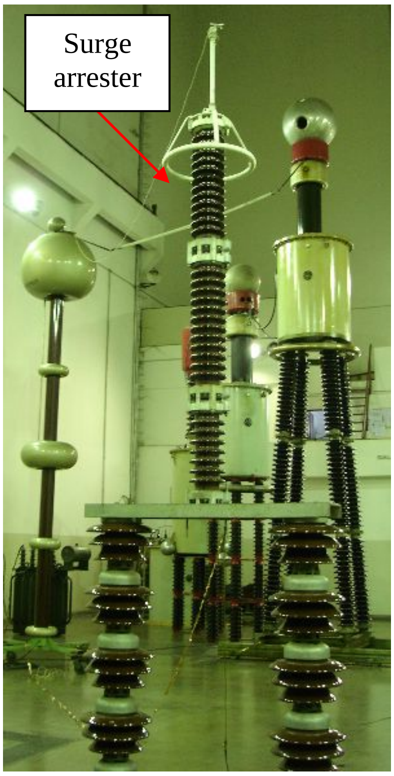

Fig.4 – Leakage current measurement in the surge arrester.

The following aspects can be pointed out, concerning the results shown in Table 3:

Manufacturer A - 88 kV surge arresters:

- all surge arresters failed the power frequency spark-over voltage test;
- surge arrester A1 presented the highest power frequency spark-over voltage value (134 kV);
- surge arrester A1, which presented the lowest amplitude value of the leakage current (0.172 mA), had the lowest 3^{a} H component (6.7 %) and the greatest phase difference (89^{0});
- on the other hand, surge arrester A4, which showed the greatest amplitude of the leakage current (0.696 mA), had the greatest 3^{a} H component (32.9 %) and the lowest phase difference (47^{0});
- surge arresters A5 and A6 presented 3^{a} H values equal to 5.7 % and 5.0 %, respectively. However, they also had smaller phase difference values;
- surge arrester A6 presented high RIV values (8,033 μV).

Manufacturer A – 138 kV surge arresters:

- all surge arresters failed the power frequency spark-over voltage test;
- surge arrester A7, which presented the highest power frequency spark-over voltage value (193 kV), also had the lowest harmonic distortion (2.6 %) and the greatest phase difference (85^{0});
- significant results were not observed in the RIV and thermovision measurements.

Manufacturer B – 138 kV surge arresters:

- all surge arresters were successful in the power frequency spark-over voltage tests;
- surge arresters B6 and B7 presented harmonic distortion values (8.5 % and 9.4 %, respectively) greater than the values obtained with other surges arresters of the same manufacturer. Smaller phase difference values were also obtained (63^{0} and 53^{0}, respectively);
- significant results were not obtained in the RIV and thermovison measurements.

Manufacturer C – 138 kV surge arresters:

- surge arrester C5 failed the power frequency spark-over voltage test and presented 3ª H component of 7.5 % and phase difference of 83^0;
- although surge arrester C6 was succesful in the power frequency spark-over voltage test, it presented leakage current amplitude of 0.726 mA, distortion of 18 % and phase difference of 51^0, which may indicate some degradation of its internal components;
- surge arresters C5 and C6 had high RIV values, suggesting the presence of internal electrical discharges. In spite of this, the thermovision measurement showed higher temperature only in surge arrester C6.

Manufacturer D – 138 kV surge arresters:

- surge arresters D3 and D5 failed the power frequency spark-over voltage test;
- surge arrester D5, which presented the lowest power frequency spark-over voltage value, had the greatest leakage current distortion (3.8 %) and the smallest phase difference (78^0);
- significant results were not observed in the RIV and thermovision measurements.

3 Conducted Electromagnetic Field

The presence of internal electrical discharges can be detected by RIV measurements in the surge arrester. However, it is very difficult to perform this measurement at the substation due to the noisy environment in the vicinity of the surge arrester. Then, a new approach was used bearing in mind the identification of SiC surge arresters that could present internal electrical discharges in the substation.

In order to verify the feasibility of this technique, a phase-to-ground voltage of 80 kV (service voltage) was applied to the C5 surge arrester at the laboratory. This arrester presented a high level of RIV (4,518 μV), as shown in Table 3. The presence of discharges in the surge arrester was intended to be detected by measuring the emission of the electromagnetic field provoked by the internal electrical discharges.

The electromagnetic field emitted from the surge arrester was measured by using a high frequency current transformer (CT) placed in the earth cable of the surge arrester.

An antenna was also used to perform the same measurement. Then, the presence of internal electrical discharges was detected by measuring either a conducted high frequency signal (CT) or emitted signal (antenna). The signal from the CT or the antenna was measured with an instrument called Spectral Analyzer, considering several ranges of frequency of the spectral analyzer.

As an example, Fig. 5 and Fig. 6 show the results related to the C5 surge arrester in the ranges of 300 kHz – 800 kHz and 1 MHz – 3 MHz, respectively. It was possible to identify the signal from the internal electrical discharges (high amplitude) and the signal from the environment (low amplitude).

Based on the results, it was concluded that the internal electrical discharges could be detected by using a high frequency CT in the substation.

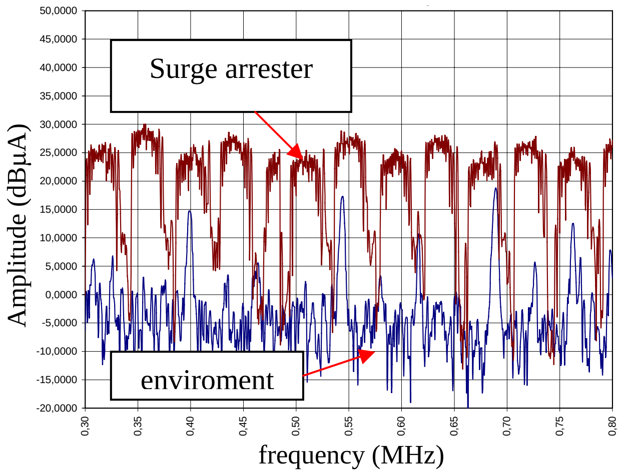

Fig.5 – High frequency signals: surge arrester C5 (300 kHz – 800 kHz).

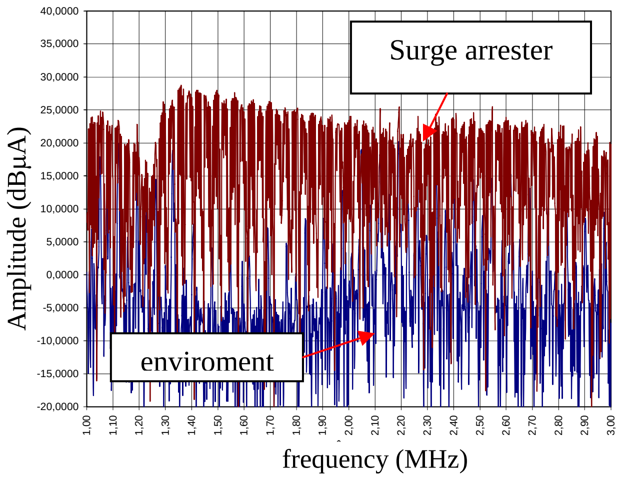

Fig.6 – High frequency signals: surge arrester C5. (1 MHz – 3 MHz).

4 Visual inspection of the internal components of the surge arrester

Some of the surge arresters were disassembled in order to investigate the presence of deterioration in their internal parts and to correlate this information with the results showed in Table 3. The following surge arresters were selected: A2, A4, A6 (manufacturer A) and C1, C3 and C5 (manufacturer C).

In the surge arresters A2, A4 and A6 there are permanent magnets in parallel with gap electrodes. Nonlinear resistors are placed between the gap electrodes. The dismantled surge arrester of manufacturer A can be seen in the Fig. 7.

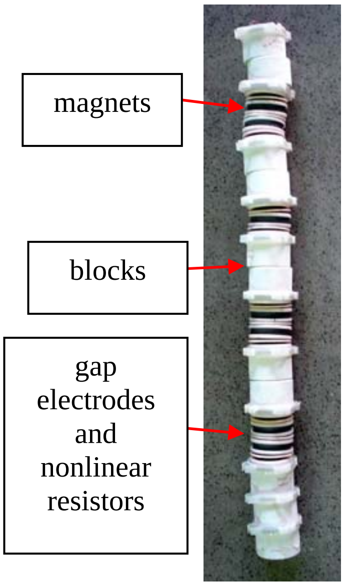

Fig.7 – Surge arrester of manufacturer A.

In the surge arresters of manufacturer C, the gap electrodes are divided in groups. In each group is applied a tape to fix the gap electrodes. A nonlinear resistor is placed in parallel with each group to equalize the voltage potential of the gap electrodes. At the edges are placed coils in order to facilitate arc extinguishing. Fig. 8 shows one group of gap electrodes.

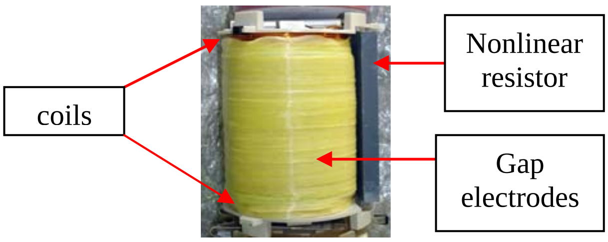

Fig.8 – Group of gap electrodes of surge arrester C.

The internal components of the surge arrester C can be seen in Fig. 9.

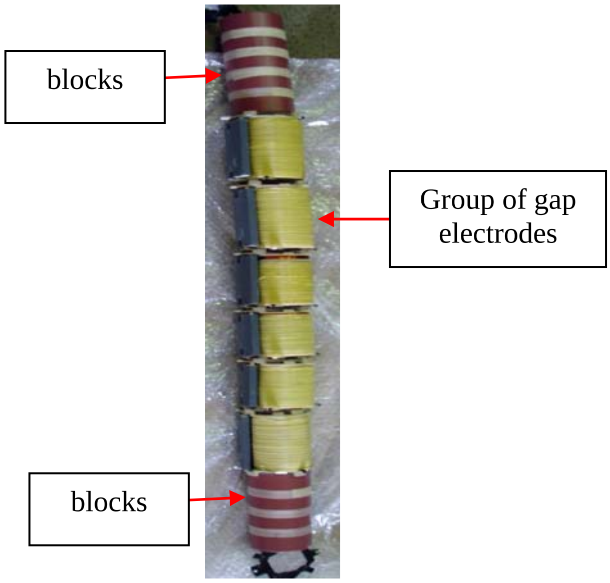

Fig.9 – Surge arrester of manufacturer C.

In general, it was noticed the presence of moisture in the surge arresters. Some traces of discharges on the surface of the blocks were also observed. Some of the surge arresters presented signs of discharges in the gap electrodes. During the visual inspection it was also observed that some nonlinear resistors were damaged.

The surge arrester A6 (manufacturer A) was more degraded in comparison with A2 and A4. The arrester C5 (manufacturer C) was the worst in comparison to the surge arresters C1 and C3.

The surge arrester C5 presented some broked nonlinear resistors and, probably, was the reason for the high level of RIV (4,518 μV), shown in Table 3. This surge arrester also failed the power frequency spark-over voltage test. In Fig. 10 and Fig. 11 it is possible to visualize the condition of the components of the surge arresters, considering manufacturers A and C.

As a general conclusion, it was observed that the surge arresters of manufacturers A and C presented evidence of ingress of moisture and signs of discharges. Afterwards, surge arresters of manufacturer B were also dismantled and it was observed that the internal components were in good condition. This results means that they could remain in service for period of time until be replaced by the ZnO surge arresters.

(a) blocks: signs of discharge.

(b) gap electrodes: signs of discharge.

(c) block: presence of moisture.

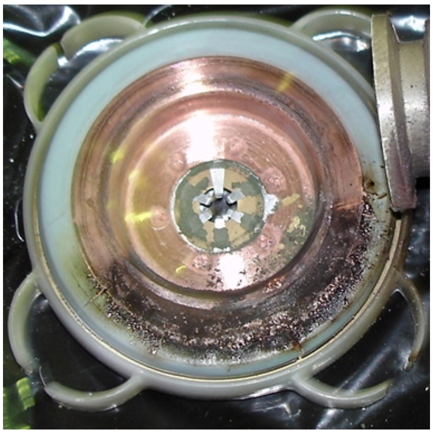

(d) gap electrode: signs of discharge.

Fig.10 – Surge arresters of manufacturer A.

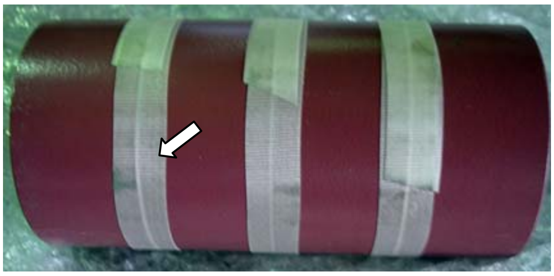

(a) block surface: presence of moisture.

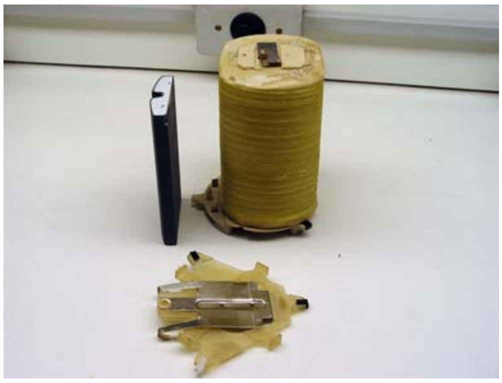

(b) group of gap electrodes: damage.

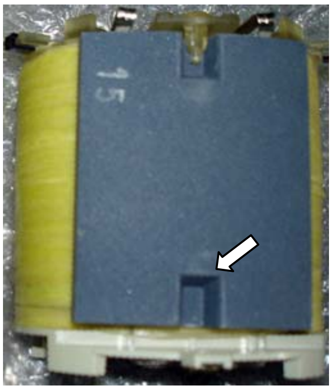

(c) nonlinear resistor: broken.

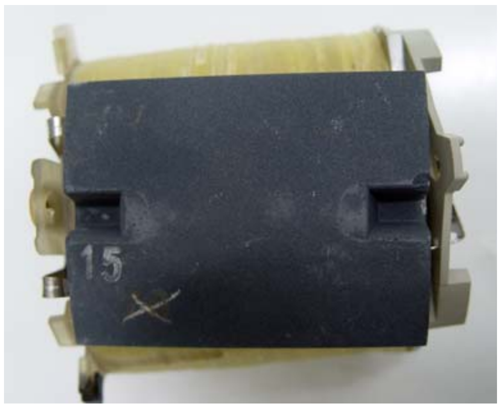

(d) nonlinear resistor: broken.

Fig.11 – Surge arresters of manufacturer B.

5 Tests of the internal components of the surge arresters

Tests were performed considering the internal components of the surge arresters A2, A4, A6, C1, C3 and C5. The aim was to compare the results obtained with the internal components and the values considering the respective surge arresters before disassembling, as shown in Table 3.

The following tests were performed:

- measurements of the 3^a H component in the nonlinear resistors;
- RIV measurements, considering the gap electrodes.

The measurement of the 3^a H component in the nonlinear resistors was performed by using the facilities, as shown in Fig. 12.

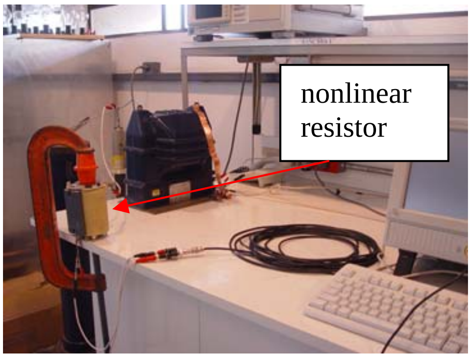

Fig.12 – Measurement of the 3^aH component.

Measurements were performed considering test voltages between 0.5 kV and 8.0 kV. Table 4 shows the results obtained with the gap electrodes of surge arrester C5, considering the test voltage of 8.0 kV.

Table 4: Results of surge arrester C5.

Group of gap electrodes	Test voltage (kV)	3^a H Component (%)
1	8.0	5,54
3		15,40
4		10,53
5		11,50

The gap electrodes number 3 presented 3^a H component higher than numbers 1, 4 and 5.

Afterwards, RIV measurements were performed in the internal components of the surge arresters. The following results are referred to the surge arrester C5. The aim was to investigate the high level of RIV (4,815 μV) measured in the surge arrester before disassembling it.

In each group of gap electrodes was applied the test voltage of 8.0 kV in order to measure the level of RIV. Fig. 13 shows the circuit used at the laboratory.

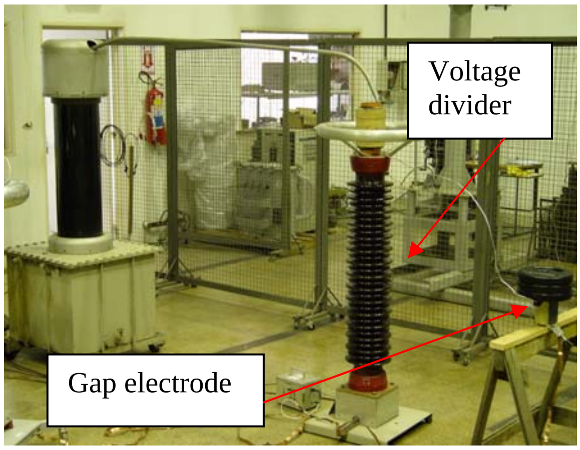

Fig.13 – Measurement of RIV.

The group of electrodes number 3 presented 2,494 μV at the test voltage of 8.0 kV. Table 5 shows the results of RIV measurements.

Table 5: RIV of internal components of surge arrester C5.

Group of gap electrodes	Test voltage (kV)	RIV (μV)
1	8.0	28
3		2494
4		20
5		5

It can be seen in Table 4 and Table 5 that the group of electrodes number 3 presented the highest 3^a H component and also the highest RIV. These results suggest the presence of internal electrical discharges in the group of electrode number 3. Probably, this is the reason of the high level of RIV in the surge arrester C5 (Table 3).

6 Conclusion

The conclusions of this research were based on laboratory tests, visual inspection and tests of the internal components of dismantled surge arresters. The evaluation of these surge arresters was conducted at the IEE/USP High Voltage Laboratory and the following tests were performed: power frequency spark-over voltage, lightning spark-over voltage and AC leakage current measurement. Thermovision and radio-influence voltage test were also performed in some arresters in order to have additional information concerning the condition of the internal components of the SiC surge arresters.

Having the laboratory tests in mind, it was observed that the presence of degradation in the surge arrester could be detected due to high leakage current and harmonic distortion (3ª H) values, high RIV values and excessive heating of the surge arrester.

The diagnosis of the condition of the surge arrester must be made carefully because one of the surge arrester succeeded in the power frequency spark-over voltage test and presented high RIV values, which indicates the existence of internal discharges. The thermovision technique, which is generally adopted by the utilities, did not detect any abnormal heating. The 3ª H component of the leakage current was slightly greater compared to the measurements of the other surge arresters of the same manufacturer.

References:

[1] M.Darveniza, M., R. Mercer and R. M. Watson, An Assessment of the Reliability of In-Service Gapped Silicon Carbide Distribution Surge Arresters, *IEEE Transactions on Power Delivery*, vol.11, nº4, October, 1996, pp. 1789-1797.

[2] Carneiro, J. C., Policy for Renewal of Power System Substations Silicon Carbide (SiC) Surge Arresters: A New Technical Economical Vision, *Proceedings of the International Symposium on Lightning Protection (SIPDA)*, Foz do Iguaçu, Brazil, 26th – 30th September, 2007, pp. 294–299.

[3] Grzybowski, S. and Gao, G., Evaluation of 15-420 kV Substation Lightning Arresters after 25 Years of Service, *Proceedings of the Southeastcon '99*, March, 1999, pp.333 – 336.

[4] McDermid W., Reliability of Station Class Surge Arresters, *Proceedings of the 2002 IEEE International Symposium on Electrical Insulation*, April, 2002. pp.320-322.

[5] IEC 60099-1, Surge arresters - Part 1: Non-Linear Resistor Type Gapped Surge Arresters for A.C. Systems – Edition 3.1 (1999).

[6] Schei, A., Diagnostics Techniques for Surge Arresters with Main Reference to On-Line Measurement of Resistive Leakage Current of Metal Oxide Arresters, *International Conference on Large High Voltage Electric Systems (CIGRÉ 2000)*, August 27 - September 1, 2000, Paris, France, pp.1-10.

[7] Almeida, C. A. L. et al., Intelligent Thermographic Diagnostic Applied to Surge Arresters: A New Approach, *IEEE Transactions on Power Delivery*, 2009, vol.24, nº 2, pp.751-757.

[8] Christodoulou, C. A. et al., Simulation of Metal Oxide Surge Arresters Behavior, *IEEE Power Electronics Specialists Conference (PESC 2008)*, Rhodes, Greece, 15–19 June, 2008, pp.1862–1866.

[9] Oonsivilai, A. and Marungsri, B., Application of Artificial Intelligent Technique for Partial Discharges Localization in Oil Insulating Transformer, *WSEAS Transactions on Systems*, Issue 10, vol.7, October, 2008, pp.920–929.

[10] Li-Xue, L. et al., Partial Discharge Diagnosis on GIS Based on Envelope Detection, *WSEAS Transactions on Systems*, Issue 11, vol.7, November, 2008, pp.1238–1247.